Title

Lipid nanoparticles loaded with butamben and designed to improve anesthesia at inflamed tissues

Journal

Biomaterials Science, 9(9)

ISSN

2047-4830

Authors

Rodrigues da Silva, Gustavo H

Lemes, Julia Borges Paes

Geronimo, Gabriela

et al.

Publication Date

2021-05-04

DOI

10.1039/d1bm00077b

Biomaterials Science

ROYAL SOCIETY OF CHEMISTRY

PAPER

View Article Online
View Journal | View Issue

Cite this: *Biomater. Sci.*, 2021, **9**, 3378

Lipid nanoparticles loaded with butamben and designed to improve anesthesia at inflamed tissues†

Gustavo H. Rodrigues da Silva, [a] Julia Borges Paes Lemes,[b] Gabriela Geronimo,[a] Fernando Freitas de Lima,[a] Ludmilla David de Moura,[a] Ariany Carvalho dos Santos,[c] Nathalia Santos Carvalho,[b] Kauê Franco Malange,[b] Márcia C. Breitkreitz,[d] Carlos A. Parada[b] and Eneida de Paula*[a]

Received 15th January 2021,
Accepted 19th February 2021

DOI: 10.1039/d1bm00077b

rsc.li/biomaterials-science

The most frequently used local anesthetics (LA) for local infiltration have an ionizable amine in the range of pH 7.6–8.9. Effective anesthesia of inflamed tissues is a great challenge, especially because the induced local acidosis decreases the fraction of the neutral (more potent) LA species *in situ*. To solve this limitation, the butyl-substituted benzocaine analogue butamben (BTB) – that has no ionizable amine group close to the physiological pH – could be useful if it was not for its low solubility. To overcome the solubility problem, an optimized formulation for BTB using nanostructured lipid carriers (NLC) was developed by a factorial design and characterized using DLS, XRD, DSC and cryo-EM. The release kinetics and cytotoxicity of the new formulation were measured *in vitro*, while the *in vivo* tests assessed its effectiveness on healthy and inflamed tissues, in rats. The optimized NLC_{BTB} formulation showed desirable physicochemical properties (size = 235.6 ± 3.9 nm, polydispersity = 0.182 ± 0.006 and zeta potential = −23.6 ± 0.5 mV), high (99.5%) encapsulation efficiency and stability during 360 days of storage at room temperature. NLC_{BTB} prolonged the release of butamben and decreased its *in vitro* cytotoxicity without inducing any *in vivo* toxic alteration. In the inflammatory hyperalgesia model, the NLC_{BTB} formulation showed potential for the management of inflammatory pain, displaying greater analgesic effectiveness (40%) and a prolonged effect.

1. Introduction

The local anesthetics (LA) currently administered using an infiltration route belong to the aminoamide family and have a pK_a between 7.6–8.9, so that both the neutral (with the largest partition in membranes) and the protonated species (which is responsible for the speed of action) are available at the physiological pH (7.35–7.45).[1,2] Indeed, at pH 7.4, most of the LA are protonated, with a small, but significant, fraction in the neutral form. Although both LA species are pharmacologically relevant, permeation of the nerve cell membrane by the neutral LA is a requisite for the protonated species to reach the binding sites of the voltage-gated sodium channels, from the inner side of the membrane.[1,3,4]

Although routinely used for pain control, specific biological conditions can cause LA to fail in blocking the nerve impulse propagation. In dentistry, for instance, anesthesia failure can reach up to 70% of patients with active inflammatory pathologies.[5] The inflammatory process causes local acidosis, and the decrease in tissue pH may be of 0.5–1 pH unit[6] reducing the (uncharged) LA fraction capable of partitioning into the membrane to trigger anesthesia. This "acidosis" theory, together with other physiological factors (*i.e.* increased local blood flow, edema and hyperalgesia) are markedly the key mechanisms responsible for anesthesia failure under inflammation.[5–9] Another relevant point is that LA are marketed as (hydrochloride) salts, in acidic solutions (pH 3–7) of increased water solubility and shelf life.[10–12] However, the injection of these salts can cause a decrease in the tissue pH,[13] worsening the inflammatory acidosis.

Nowadays, there is no effective solution to overcome the problem of anesthesia failure related to the inflammatory process.[9,14] One could think that increasing the anesthetic concentration would provide the desired antinociception, but

[a]*Department of Biochemistry and Tissue Biology, Institute of Biology, University of Campinas – UNICAMP, Campinas, São Paulo, Brazil. E-mail: depaula@unicamp.br; Tel: +551935216143*
[b]*Department of Structural and Functional Biology, Institute of Biology, UNICAMP, Brazil*
[c]*Faculty of Health Sciences, Federal University of Grande Dourados, Dourados, MS, Brazil*
[d]*Department of Analytical Chemistry, Institute of Chemistry, UNICAMP, Brazil*
†Electronic supplementary information (ESI) available. See DOI: 10.1039/d1bm00077b

higher LA doses also enhance the risk of systemic toxicity.[15] Another way to get around the problem would be using LA from the ester family (*e.g.* benzocaine and butamben) that have no ionizable groups in the range of pH 4–14.[16] However, these drugs are highly insoluble in water, their clinical use being restricted to topical anesthesia.[17] Thus, we consider developing a new drug delivery system (DDS), to be able to improve the bioavailability of butamben.

N-Butyl-*p*-aminobenzoate or butamben (BTB) is a very hydrophobic ester local anesthetic (water solubility ~140 μg L^{-1}).[18] Despite advantages such as long anesthesia time and selectivity to sensory block,[19] the limited water solubility curbs many clinical applications of BTB.[20] Nowadays, butamben is marketed only as a topical formulation (cetacaine: 14% benzocaine, 2% butamben and 2% tetracaine).[21] Suspensions were developed for parenteral application, mainly in chronic pain.[22] However, in 1998, parenteral BTB formulations were withdrawn from the market by the FDA for reasons of safety and effectiveness.[23] Unlike most of the commercialized LA agents, BTB does not undergo ionization close to the physiological pH (its amino-benzoate group has a pK_a = 2.5). Hence, BTB is always in the neutral form, which has a greater partition into membranes, either at pH 7.4 or in the acidic milieu (pH 6.4–6.9) of inflamed tissues.

Nanostructured lipid carriers (NLC) are an ideal DDS for the encapsulation of hydrophobic drugs and they are formed by a blend of solid and liquid lipids, surrounded by a surfactant.[24] These lipid nanoparticles are efficient carriers for local anesthetics, improving their time of action, with no systemic toxicity.[16] Encapsulation of BTB in the NLC could provide a soluble, injectable formulation for this topical anesthetic agent, overcoming the problem of anesthesia failure at the inflamed tissues and even increasing BTB effectiveness by promoting a sustained delivery at the application site.

From this perspective, a novel NLC formulation containing butamben was developed and optimized using factorial design. The optimized NLC_{BTB} formulation was characterized by DLS, cryo-TEM, DSC and XRD, and its shelf stability was followed for 360 days. *In vitro* release and cytotoxicity tests were performed with the optimized formulation. Furthermore, using the carrageenan-induced inflammation model *in vivo*, anesthesia tests (sciatic nerve blockage in rats) were conducted to assess the performance of the formulation in the inflamed tissues. Concomitant evaluation of biochemical and histological parameters allowed the assessment of the local and systemic toxicity of NLC_{BTB}. From our knowledge, this is the first report of a lipid-based DDS for butamben, and it successfully improved the anesthetic effect, after parenteral administration.

2. Materials and methods

2.1. Materials

Butamben (BTB), Pluronic F-68 (P68), Tween 80 (T80), DMEM medium, fetal bovine serum, 3-(4,5-dimethylthiazol-2-yl)-2,5-diphenyltetrazolium bromide (MTT) and λ-carrageenan were supplied by Sigma-Aldrich (St Louis, MO, USA). The lipids cetyl palmitate (CP) and Dhaykol 6040 LW (DK, a blend of caprylic/capric acid triglycerides) were donated by Dhaymers Química Fina (São Paulo, Brazil). Deionized water (18 MΩ) was obtained from an Elga USF Maxima ultra-pure water purifier. All other reagents were of analytical grade.

2.2. NLC preparation

To produce the NLC, an ultrasonication method[25] was used. Briefly, CP, DK and BTB were melted at 65 °C in a water bath and a solution of P68 was heated to the same temperature. Both phases were blended under high-speed agitation (10 000 rpm) for 3 min in an Ultra-Turrax homogenizer (IKA Werke, Staufen, Germany). After that, the mixture was sonicated for 10 min using a Vibracell tip sonicator at 20 kHz/500 W (Sonics & Mat. Inc., Danbury, USA), in alternating 30 s (on/off) cycles. The resultant nanoemulsion was immediately cooled to room temperature in an ice bath to form the nanoparticles.

2.3. Factorial design (FD)

A 2^3 factorial design with central points in triplicate was performed using Design Expert software (version 10, Stat-Ease Inc., USA). Analysis of Variance (ANOVA) was applied to verify the regression significance and identify the most important experimental variables (p-value <0.05).[26] The variables and levels are listed in Table 1, as well as the optimization criteria applied to the analyzed responses such as nanoparticle size, polydispersity index (PDI) and zeta potential (ZP).

2.4. Characterization

2.4.1. Size, PDI and zeta potential. A Nano ZS90 analyzer (Malvern Instruments, UK) was used to determine the nanoparticle size and polydispersity by dynamic light scattering (DLS) and the zeta potential by laser Doppler microelectrophoresis. All the analyzed samples were diluted in deionized water (1000×, n = 3). To follow the shelf stability, these parameters were also monitored in the formulations optimized by factorial design, during 360 days of storage, at room temperature.

2.4.2. Butamben quantification and encapsulation efficiency determination. Butamben was quantified using high-pressure liquid chromatography (HPLC), Waters Breeze 2 (Waters Technologies, Milford, MA, USA) equipment and a C18 Gemini-NX, 5μ, 150 × 4.60 mm column, at 35 °C. The

Table 1 Experimental variables, levels and responses analyzed in the 2^3 factorial design

Variables	Symbols	Low level	High level
Total lipids (TL, % w/w)	A	10	15
P68 (% w/w)	B	4	6
BTB (% w/v)	C	3	5
Responses	**Optimization**		
Size (nm)	Lowest		
PDI	<0.2		
ZP (|mV|)	>20		

mobile phase was a mixture of methanol : water 70 : 30 (v/v), applied at 1 mL min^{-1} flux. The detection was followed at 290 nm. The limit of detection and quantification of the analytical method were 0.78 μg mL^{-1} and 2.60 μg mL^{-1}, respectively. The encapsulation efficiency (%EE) of BTB by the nanoparticles was determined by the ultrafiltration–centrifugation method, using cellulose filters (30 kDa, Millipore). Briefly, the total amount (100%) of butamben in the NLC was determined (BTB_{total}) by diluting the samples in the mobile phase (n = 3). The amount of BTB in the filtrate (BTB_{free}) was quantified by HPLC and the percentage of encapsulated BTB was calculated according to eqn (1):[27]

$$\%EE = \frac{BTB_{total} - BTB_{free}}{BTB_{total}} \times 100 \quad (1)$$

2.4.3. Cryogenic electron microscopy (Cryo-EM). Cryo-EM was performed at the National Laboratory of Nanotechnology (LNNano, at CNPEM, Campinas, SP). A 300 mesh holey lacey carbon grid from TedPella was used, and the grid was subjected to a glow discharge procedure (Pelco easiGlow discharge system-Ted Pella, USA) of 20 mA for 10 s to make it more hydrophilic. Afterwards, the grid was inserted in a Vitrobot® (Mark IV, Thermo Fisher Scientific, USA), where 3 μL of the sample were added and left for 20 s for sample fixation. Subsequently, an automatic blotting (3 s) was performed to dry the sample excess, with a negative blotting force (blot force = −5). Finally, the grid was rapidly plunged into liquid ethane wrapped in a liquid nitrogen environment. Images were obtained using a Talos F200 (Thermo Fisher Scientific, USA) microscope at 200 kV with dedicated software for micrograph acquisition. ImageJ 1.52a software[28] was used to estimate the sizes of the NLC in the micrographs. In that case, 20 nanoparticles, from two different images, were analyzed, per sample.

2.4.4. Differential scanning calorimetry (DSC) and X-ray diffraction analysis (XRD). A 2910 TA calorimeter with Thermal Solutions v.1.25 software (TA Instruments, DE, USA) was used to acquire the DSC thermograms; the samples were placed in a hermetic aluminium pan and heated/cooled at the rate of 10 °C min^{-1}, in the temperature range of 20–150 °C. The analysed samples were: CP, BTB, P68 and the freeze-dried samples of nanoparticles, without (NLC_{ctrl}) and with (NLC_{BTB}) BTB.

Powder X-ray diffraction (XRD) data were obtained using a Shimadzu XRD7000 diffractometer (Tokyo, Japan), using a Cu-Kα source. Diffractograms were obtained between 2θ values (5 and 50°), at a scan step of 2° min^{-1} for the samples: CP, BTB, freeze-dried NLC_{CRTL} and NLC_{BTB}.

2.5. *In vitro* tests

2.5.1. Release kinetics experiment. The *in vitro* release of BTB was monitored using 12 mL Franz diffusion cells, at 37 °C, 350 rpm. A cellulose dialysis membrane (Spectro/Por, MWCO 12–14 kDa) separated the acceptor and receptor chambers. The receptor medium was a solution of 30% propylene glycol, in which BTB solubility was determined to be 1.45 ± 0.02 g L^{-1}. The samples (50 μL; 1.5 mg) containing 3% BTB were added to the donor compartment. Three samples were tested: free BTB = butamben dissolved in a solution of 70% propylene glycol (BTB solubility = 40.6 ± 0.03 g L^{-1}), SUS_{BTB} = butamben suspended in 2.5% polyethylene glycol and 0.025% Tween 80,[18,29] and NLC_{BTB} = butamben loaded in NLC. At settled intervals (0.15, 0.3, 1, 2, 4, 6, 8, 22, 24 and 28 h), 200 μL aliquots were collected from the sampling port of the receptor chamber, and this volume was replaced with a fresh medium to maintain the sink conditions (n = 6). The amount of BTB in the aliquots was quantified by HPLC.

For the quantitative analysis of the release curves obtained, we used KinetDS 3.0 software.[30] Several kinetic models were tested, and according to the R^2 coefficient, the Weibull model[31] (eqn (2)) showed the best fit for the curves of SUS_{BTB} and NLC_{BTB}:

$$m = 1 - \exp\left[\frac{-t^n}{a}\right] \quad (2)$$

where m is the amount of BTB released as a function of time (t), a is the scale parameter that describes the time dependence and the shape, and n characterizes the curve.

2.5.2. Cell viability assay. RSC96 (ATCC® CRL-2765™) is a spontaneous immortalized neuronal Schwann cell lineage from *Rattus norvegicus.* The cells were cultured in a DMEM medium and supplemented with 10% fetal bovine serum and 1% antibiotic (100 IU mL^{-1} penicillin and 100 μg mL^{-1} streptomycin sulfate). The cells were plated in 75 cm^2 bottles and incubated at 37 °C under a humidified 5% CO_2 atmosphere for 48 h, until semi-confluence. To assess the cell viability, the MTT method was used. Briefly, the cells (4×10^4 cells per mL) were plated in 96-wells for 24 h. After this period, the culture medium was replaced with samples (0.1, 0.25, 0.5, 0.75, 1, 2, 3, 4 and 5 mM) of BTB (in solution – dissolved in a solution of 70% propylene glycol and NLC_{BTB}) and the controls (NLC_{CRTL} and propylene glycol) diluted in the supplemented DMEM medium and the cells were incubated for 2 h. After that, the medium was removed, washed with 5 mM PBS and the cells were incubated with MTT for 3 h. Then, the medium was removed, and ethyl alcohol was used to dissolve the formazan crystals produced by MTT reduction; the plates were vigorously shaken and the absorbance was measured at 570 nm.[32] The obtained results were expressed as percent cell viability (in comparison with the control) and analyzed using GraphPad Prism 6.0 software. Statistical analyses were performed by one-way ANOVA with Tukey–Kramer post-test.

2.6. *In vivo* tests

2.6.1. Animal care. Adult male Wistar rats (*Rattus norvegicus albinus*) (200–250 g) were obtained from CEMIB (Centro de Bioterismo/UNICAMP). The experimental protocol was approved by the Institutional Animal Care and Use Committee (UNICAMP protocol #4831-1) that follows the recommendations of the Guide for the Care and Use of Laboratory Animals. Rats were housed in groups of 4 individuals, with 12 h light–dark cycles with food and water *ad libitum*. All

animal procedures were conducted in accordance with the rules established by the International Association for the Study of Pain.

2.6.2. Sciatic nerve blockage (PWTP test). The rats were randomly divided into batches of 5 animals, which were treated with 0.2 mL of 3% BTB – in suspension (SUS_{BTB}) or encapsulated (NLC_{BTB}) – or the controls without BTB (SUS_{CRTL} and NLC_{CTRL}) injected posterior to the knee joint, in the sciatic nerve area.[33] Sensory blockade evaluation was performed by the paw pressure test[34] using an Ugo Basile (Varese, Italy) analgesiometer. The withdrawal reflex was considered representative of the pain threshold or Paw Withdrawal Threshold to Pressure (PWTP), taking into account the registered force (in grams) on the injected paw. The baseline of the PWTP test was measured before the injections, in order to determine the pain threshold of the animal. Baseline values of 30–50 g were selected as the pain threshold, and animals with lower or higher values than the baseline were excluded. The established nociceptive cut-off value of 180 g was considered representative of anesthesia. After the treatment, the first measurement was carried out at 30 min, and after that, in intervals of one hour, until 28 h. The obtained values were transformed into data of the maximum possible effect (% MPE) according to eqn (3):[35]

$$\%\text{MPE} = \frac{(\text{threshold} - \text{baseline})}{(\text{cutoff} - \text{baseline})} \times 100 \quad (3)$$

where the threshold corresponds to the pressure values, the baseline is the standard pressure value of each animal, and the cutoff refers to the limiting (180 g) pressure to avoid skin injury. The area under the curve (AUC) of the anesthetic effect was calculated from the %MPE plot. Statistical analyses were performed by one-way ANOVA with Tukey–Kramer post-test, using GraphPad Prism version 6.00 for Windows (California, USA).

2.6.3. Toxicological profile

2.6.3.1. Biochemical analyses. At the end of the sciatic nerve blockage test, the animals were euthanized, and blood samples were immediately collected by cardiac puncture and centrifuged (1500*g*, 15 min) using a Fanem Excelsa Baby centrifuge (São Paulo, Brazil). The obtained sera were biochemically analyzed for the markers of muscular (total and cardiac creatine kinase – CK-total and CK-MB) and liver damage (alanine and aspartate aminotransferases – ALT and AST, respectively, and alkaline phosphatase – ALP), using Beckman Coulter reagents in an AU5800 Beckman Coulter (Brea, USA).

2.6.3.2. Histopathological analyses. After blood collection, the tissue near the injection place was removed for morphological analysis of the sciatic nerve and gastrocnemius muscle. The tissues were fixed in 10% formaldehyde, cut and dehydrated with increasing absolute ethanol concentrations. The dehydrated tissues were diaphonized in xylene and embedded in paraffin. The sections (5 μm thickness) were cut, stained with hematoxylin/eosin and mounted on glass slides for observation under a light microscope.[36] The presence of inflammatory infiltrate (mononuclear and neutrophilic), edema, hemorrhage or necrosis was analyzed, and for each parameter, a 0–4 score value was assigned, where 0 = normal; 1 = minimal; 2 = slight; 3 = moderate; and 4 = substantial injury, as adapted from ref. 37 and 38.

2.6.4. Carrageenan-induced inflammatory hyperalgesia model. Rats (n = 6) received a single intraplantar injection of carrageenan (100 μg/50 μL/paw) for the induction of inflammatory hyperalgesia. The mechanical nociceptive threshold was measured by the electronic von Frey method under basal conditions (before inflammatory stimulation) and at times of 1, 2, 3, 4, 5 and 6 h post-carrageenan application. The formulations applied were: 0.5% BTB in suspension (SUS_{BTB}), 0.5% BTB in the NLC (NLC_{BTB}), and their respective controls without the anesthetic: SUS_{CTRL} and NLC_{CTRL}. Additional controls: articaine hydrochloride (0.5% ART) and saline (0.9% NaCl) were also used. All substances were injected 170 min after carrageenan administration, also by the intraplantar route. Statistical analyses were performed by two-way ANOVA with Tukey–Kramer post-test, using GraphPad Prism version 6.00 for Windows (California, USA).

2.7.4.1. Nociceptive paw electronic pressure-meter test for rats. The mechanical nociceptive threshold was measured trough the electronic von Frey method, as previously described.[39] Briefly, rats were acclimatized in a quiet room and placed in acrylic cages (12 × 20 × 17 cm) with wire grid floors, for 60 min before the tests. A tilted mirror, placed under the grid, was used to provide a clear view of the rat hind paw. The test consisted of provoking a paw withdrawal reflex using a hand-held force transducer (EFF 301A digital analgesiometer (Von Frey), Insight, Brazil) with a 0.5 mm^2 polypropylene tip applied to the metatarsal footpad. The stimulus was repeated three times and the arithmetic mean of the 3 responses was considered the mechanical withdrawal threshold (g) of the animal. For all experiments, the baseline and post-treatment measures were taken. The intensity of hyperalgesia was taken from the change in the mechanical threshold (Δ, grams), calculated by subtracting the baseline value from that measured after the treatment.

3. Results and discussion

3.1. Factorial design

In the first step of the NLC development, studies were carried out to determine the composition capable of stabilizing the drug, and the lipids cetyl palmitate (CP) and Daykol (DK) were selected to be used with the Pluronic F-68 (P68) surfactant. It is worth mentioning that the other surfactants evaluated (Tween 80 and Tween 20, 5% w/w) were not able to produce stable formulations with the same lipid excipients. Next, the appropriate amounts of each component as well as their influence on the physical properties (size, PDI and ZP) of the nanoparticles were determined using a 2^3 factorial experimental design. From 11 experimental combinations (Table S1†), it was possible to produce significant linear mathematical models

(evaluated by ANOVA) without a lack of fit that described the influence of the formulation excipients, as well as their interactions on the properties of interest, as summarized in Table 2 and as shown in the response surface graphs in Fig. 1. It is noted that the edges of the response surfaces in Fig. 1A–C are not parallel, which means that there are interactions between the variables (*i.e.*, the change in the response obtained by varying the level of one factor depends on the level of another factor), justifying the use of multivariate methodology.

As expected for the size response, the P68 surfactant had a negative effect (the increase in P68 concentration caused a decrease of response), by reducing the surface tension between the lipid and the aqueous phase, thus leading to the formation of smaller nanoparticles.[40–43] P68 interaction with BTB also contributed with a negative effect. The interaction between the three components (total lipids, P68 and BTB) had a positive contribution to the model. BTB and its interaction with total lipids were responsible for decreasing the PDI, providing a narrower size distribution. This finding differs from a previous study, where only the surfactant played a main role in the homogenization of NLC diameters.[27,44] Regarding the zeta potential, which reflects the magnitude of the electrostatic repulsion or attraction between the particles,[45,46] while TL increased the ZP values (in modulus), P68 had the opposite

Table 2 Significant positive and negative effects on the properties of interest in the 2^3 experimental design for butamben loaded in NLC. A = TL; B = P68; C = BTB

Properties of interest	Positive effect	Negative effect
Size	ABC	B and BC
PDI	—	C and AC
Zeta potential	A and AB	B

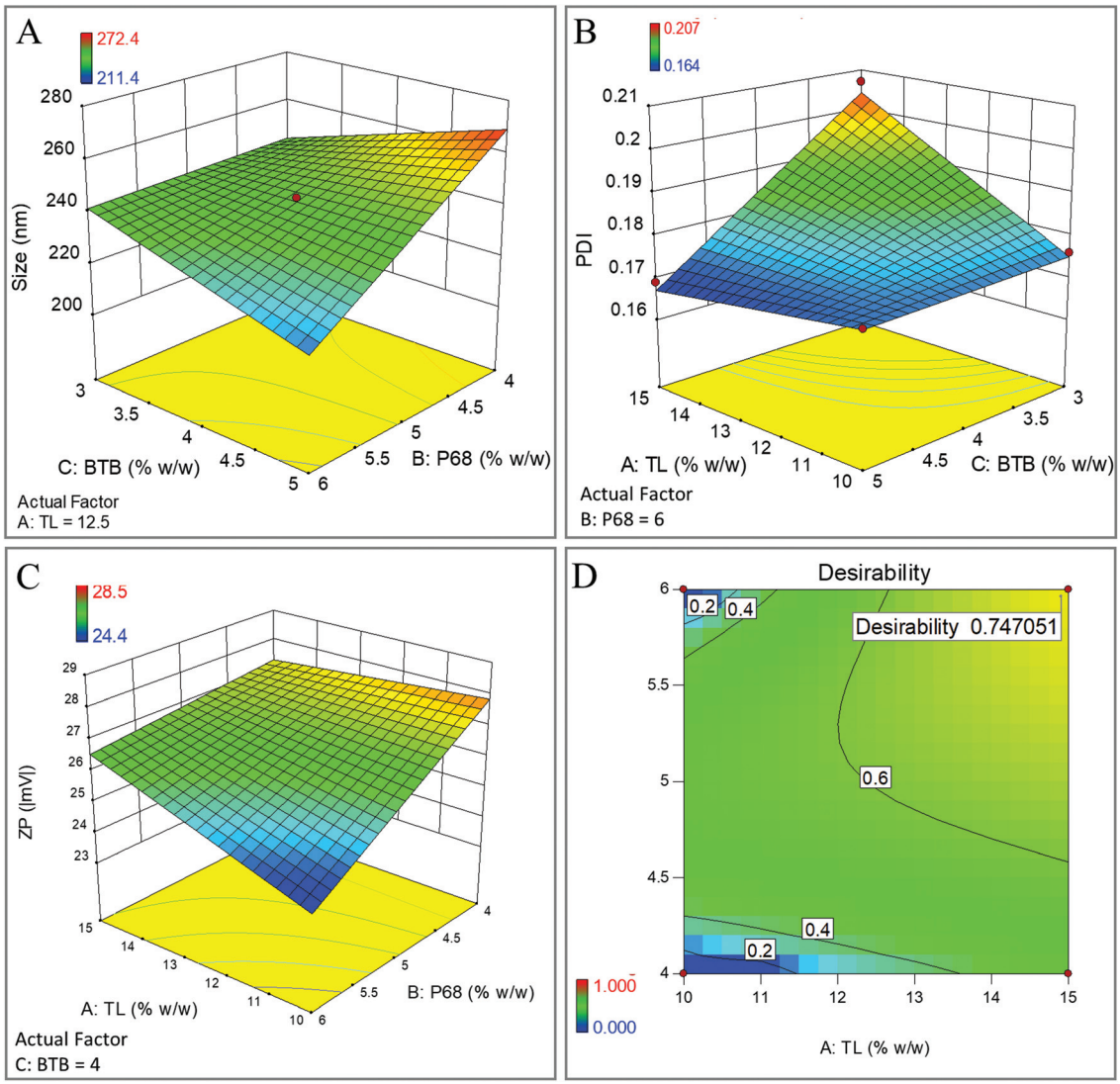

Fig. 1 Surface graphs for the studied responses as a function of the significant variables: (A) particle size; (B) PDI and (C) zeta potential. (D) Desirability graphic for the tested NLC containing butamben.

effect. Since P68 is a nonionic surfactant, a steric effect on the nanoparticle surface, followed by water adsorption, could have caused the decrease of ZP values.[47–49] Still, in all formulations, the ZP values were greater than |−20| mV, enough to ensure the stability of the NLC.[50]

From the significant mathematical models generated for each property of interest, a desirability graph (Fig. 1D) was plotted, seeking the following criteria: (1) smaller size (preferred for liquid, injectable, formulation);[51] (2) lower polydispersity index (PDI < 0.2), indicating a monodisperse particle size distribution[50] and (3) maximum ZP, in modulus. Thus, the optimized formulation chosen for BTB encapsulation was composed of 15% total lipids, 6% Pluronic F-68 and 3% butamben.

Table 3 Physicochemical characterization of the optimized formulation with (NLC_{BTB}) and without (NLC_{CTRL}) butamben

Formulation	Size (nm)	PDI	Zeta potential (mV)	%EE
NLC_{BTB}	235.6 ± 3.9	0.182 ± 0.006	−23.6 ± 0.5	99.5 ± 0.6
NLC_{CRTL}	221.9 ± 2.6	0.186 ± 0.019	−28.3 ± 0.2	—

3.2. Physicochemical characterization of the optimized formulation

The optimized formulation (NLC_{BTB}) and its control without BTB (NLC_{CTRL}) were prepared and the results of their analyses by DLS plus %EE are given in Table 3. It is noted that in relation to the control NLC, the particle size increased with the addition of BTB, while the PDI did not change and the ZP values decreased. These data suggest that BTB got inserted in the lipid core of the nanoparticles. Indeed, the encapsulation efficiency of the nanoparticles (99.5%) was excellent and confirmed the high hydrophobic character of BTB.[21]

Cryo-electron microscopy (Cryo-EM) provides a detailed visualization of the morphology of NLC.[52] When observed using this technique, both samples, with and without BTB, showed circular and ellipsoidal structures (Fig. 2A and B) with weak borders that are characteristic of NLC.[53] In addition, the mean particle sizes estimated from the Cryo-EM micrographs with the help of ImageJ software (Fig. 2C) were coherent to

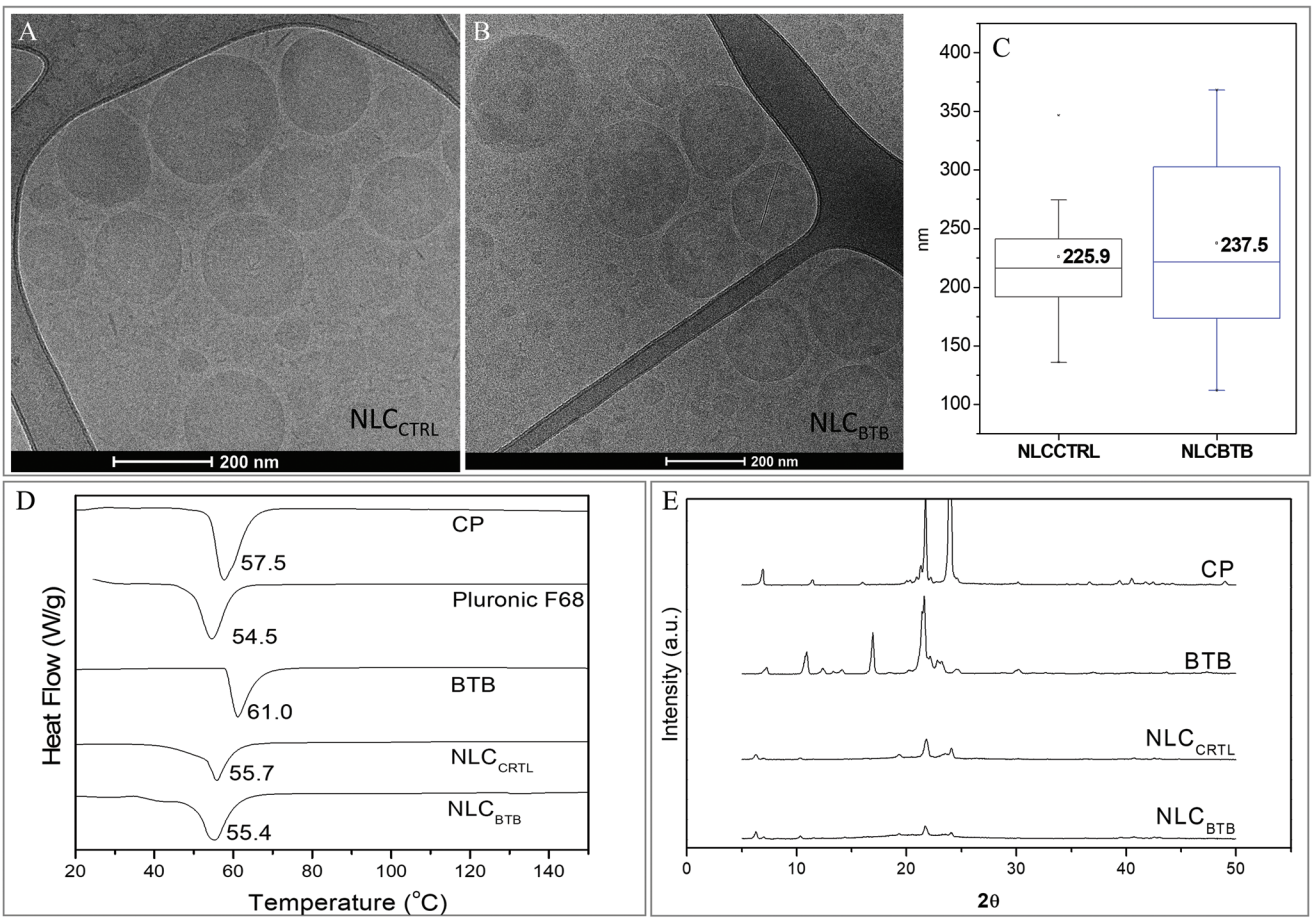

Fig. 2 Cryo-EM micrographs of the nanostructured lipid carrier without (A) and with (B) butamben. (C) Average size of NLC, determined from the Cryo-EM images, using ImageJ software. (D) DSC thermograms, obtained at a heating rate of 10 °C min^{-1}. (E) X-ray diffractograms obtained with a Cu-Kα source, at a scan step of 2° min^{-1}, for the samples: cetyl palmitate (CP), butamben (BTB), and the optimized nanostructured lipid carriers without (NLC_{CRTL}) and with (NLC_{BTB}) butamben.

those measured by DLS (<2% difference, for both NLC_{CRTL} and NLC_{BTB}) ensuring the reliability of the data.

DSC and XRD are complementary techniques used to study the crystalline structure of NLC.[52] Fig. 2D shows the thermograms of the excipients, plus that of the optimized NLC, while Table S2† lists the results of their melting points and enthalpy. The melting temperature of the nanoparticle's major excipients CP (transition temperature: 57.7° C) and P68 (transition temperature: 54.5 °C) are close, and therefore a unique thermal event of the intermediate temperature (55.4 °C) was observed in the NLC_{CRTL} sample. The melting point of BTB was registered at 61 °C, in accordance with the literature;[54] when inserted in the nanoparticles (NLC_{BTB}), just one exothermic transition was observed, with a slight decrease in the transition temperature (55.2 °C) and an enthalpy decrease (from 133.5 to 108.6 J g^{-1}) relative to BTB. Similar results in relation to the melting point and enthalpy were found by other authors when encapsulating hydrophobic drugs in NLC.[55,56]

The results of X-ray diffraction (Fig. 2E) reveal information on the crystallinity of the NLC lipid core.[57] Therefore, cetyl palmitate, the main lipid excipient and responsible for the solid core of the nanoparticles, showed intense peaks at 7, 11, 21 and 24°,[58] indicating its crystalline structure. Nevertheless, the intensity of these CP peaks decreased in NLC_{CRTL}, and even more in NLC_{BTB}, indicating a reduction in the crystallinity of the nanoparticle core, which contributes to the stability of the optimized system.

Indeed, the shelf stability of the optimized system was followed for a year, at room temperature, and excellent results were obtained, with no statistical differences in the size, PDI and ZP values (Fig. S1†) compared to the initial value. The low crystallinity of the NLC lipid core explains the long-term stability observed, enabling the use of this formulation in *in vitro* and *in vivo* tests.

3.3. *In vitro* tests

3.3.1. Release kinetics tests. The release kinetics profile of local anesthetics in NLC can provide information about its encapsulation and release mechanism.[44,59] The *in vitro* release curves for butamben in a solution of 70% propylene glycol (free BTB), in suspension (SUS_{BTB}, see Materials and methods) or encapsulated in the nanoparticles (NLC_{BTB}) were determined at 37 °C (Fig. 3A). Free BTB and SUS_{BTB} were used because of the low aqueous solubility of butamben. Free BTB showed 100% release after 4 h of the experiment, followed by SUS_{BTB} (8 h), while NLC_{BTB} promoted a sustained release for up to 36 h.

Due to the high hydrophobicity of butamben, its release from the lipid core of NLC was extremely slow, not showing the burst release normally observed with other water-soluble local anesthetics such as lidocaine, prilocaine and bupivacaine.[27,44] The release curves were analyzed according to different mathematical models using the KinetDS program. The best model (higher R^2) to describe the release profile from the optimized NLC, free BTB and SUS_{BTB} was the Weibull model (Table S3†).

For NLC_{BTB}, three phases can be seen in Fig. 3A: an initial (up to 2 h), characterized by a slow release, followed by a second one (up to ~8 h) with an increased release and a third phase – of slower release – that lasts till the end of the experiment. In relation to SUS_{BTB}, only the first phase was similar to NLC_{BTB}; after that, SUS_{BTB} presented a faster release. Probably, the high affinity of BTB for the lipid core of the NLC (despite the experiment being conducted under the sink conditions) caused the delay of BTB release in relation to the controls (free BTB and SUS_{BTB} samples). Although we used a solubilizing agent (propylene glycol) in the receptor medium, BTB release from the NLC took longer (36 h) than the time observed with other NLC loaded with LA of greater water solubility such as

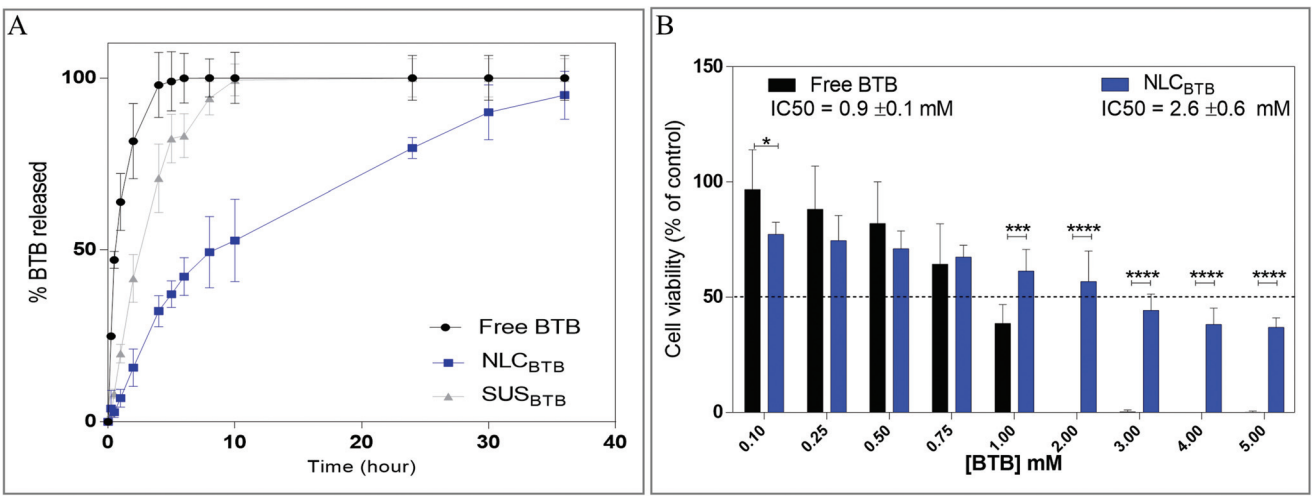

Fig. 3 *In vitro* tests. (A) Release profile of 3% butamben: in propylene glycol (free BTB), in suspension (SUS_{BTB}) and incorporated in the NLC (NLC_{BTB}), measured in Franz cells at 37 °C (n = 6). (B) Cell viability of the neuronal Schwann cells (ATCC® CRL-2765) treated for 2 h with butamben in propylene glycol (free BTB) and encapsulated in the NLC (NLC_{BTB}). Statistical analysis by two-way ANOVA plus Tukey–Kramer *post hoc* test. *p < 0.05, ***p < 0.001; ****p < 0.0001.

lidocaine and prilocaine (*ca.* 24 h)[44,58] or bupivacaine (28 h),[27] confirming the higher affinity of BTB for the NLC lipid core.

3.3.2. Cell viability tests. Local anesthetics show intrinsic and dose-dependent cytotoxic effects.[60,61] NLC are poorly cytotoxic, depending on the lipid matrix composition.[62–64] Fig. 3B shows the cell viability results obtained with rodent Schwann cells treated with BTB, either free or encapsulated (NLC_{BTB}), confirming their dose-dependent cytotoxicity.[21] The IC_{50} value (concentration that reduces the cell viability by 50%) with free BTB (0.9 mM) increased in the cells treated with NLC_{BTB} (2.6 mM), showing that encapsulation decreased the cytotoxicity caused by BTB – an encouraging result foreseeing the *in vivo* delivery of BTB. Besides, the solvent (propylene glycol) used to solubilize butamben in the control (free BTB) sample did not show any cytotoxicity at the concentrations tested (Fig. S2†). Lastly, Fig. S3† shows that NLC_{CRTL} promoted a slight decrease in the cell viability (IC_{50} > 5 mM), possibly due to its excipients,[62] but less pronounced than that induced by BTB, the most toxic compound for the Schwann cells in the tested concentrations.

3.4. *In vivo* tests

3.4.1. Sciatic nerve blockage and toxicological tests. The *in vivo* antinociceptive effect of the formulation was evaluated by the sciatic nerve blockage in rats, through the paw-pressure test (PWTP), a well-described technique to study the anesthetic action.[65] Fig. 4A shows that the maximum possible effect (MPE) evoked by the formulations was reached 1 hour post injection. After that, with the SUS_{BTB} sample, the effect decreased slowly, until the end of experiment (*ca.* 24 h), with 70% MPE at 10 h. NLC_{BTB} evoked a similar profile of anesthesia, but the antinociceptive effect remained longer near the maximum: 90% MPE after 10 h post injection. This is clearly seen in Fig. 4B, which shows the effect × time relationship in terms of the area under the curve (AUC). According to this, NLC_{BTB} surpassed the effect of SUS_{BTB} by 40% ($p < 0.05$). This result clearly indicates better delivery of butamben at the site of action as a result of its encapsulation into the optimized DDS.[16,59] Although there is a report in the literature claiming that 5% SUS_{BTB} provided an ultralong antinociceptive effect (17 days), as assessed by the hot plate test in rats,[29] we show here, through the PWTP test, that 3% BTB in the optimized NLC formulation elicited one day of anesthesia. This duration was twice as long as that observed with bupivacaine – a long-term anesthetic and the global drug-of-choice for surgical procedures – in NLC;[27] a plausible result since the time-of-action is proportional to the hydrophobicity of the LA agent.[16]

During the development of new DDS, it is important to obtain information on the possible systemic and tissue toxicity of the formulation.[66,67] For this purpose, after the sciatic nerve blockage test, the blood of the rats was collected by cardiac puncture to access possible toxic effects of the nanoparticles at specific tissues. Levels of creatine kinase (total, CK-total, and its isoform CK-MB), alanine aminotransferase (ALT), aspartate aminotransferase (AST) and alkaline phosphatase (ALP) were measured, and results are given in Fig. 4C. The levels of CK-total and CK-MB – known markers of myocyte injury such as in acute myocardial infarction and myocarditis – did not show statistical difference when the SUS_{BTB}, NLC_{CRTL} or NLC_{BTB} group was compared to the control group (SUS_{CRTL}). This result indicates the absence of muscle/myocardial damage, a well-known undesirable effect of LA.[68] No significant alterations were observed in the activity of ALT, AST, and ALP, enzymes that are markers of liver injury. Since after administration NLC could accumulate in the liver for degradation,[69–71] these results confirmed that the formulations caused no damage to the hepatic tissue after a single dose administration, in the time tested. In the same way, Pokharkar and co-workers, following 28 daily administrations of NLC formulations, no changes were found in the ALT and AST levels.[72]

In addition to systemic toxicity, tissue damage was accessed through histopathological analysis of the sciatic nerve and skeletal muscle, near the application site. The score of damage and its frequency in the samples are given in Table S4.† No histopathological changes were observed in the sciatic nerve (Fig. 4D and E) or in the striated skeletal muscle around it (Fig. 4H and I) of animals treated with the suspension formulations without (SUS_{CTRL}) or with BTB (SUS_{BTB}), but for one animal, in which the SUS_{BTB} sample induced mononuclear inflammatory infiltrate on both tissues (Table S4†). This result is in agreement with those reported by McCarthy and colleagues where BTB in suspension caused minimal histological findings, even after 10 days of administration.[29]

In contrast, the nanoparticle groups (NLC_{CRTL} and NLC_{BTB}) showed considerable values of mononuclear inflammatory infiltrate (MII), neutrophilic inflammatory infiltrate (NII) and edema (Table S4†). In the sciatic nerve, both the NLC_{CRTL} and NLC_{BTB} formulations showed MII score 3, NII score 1 and edema score 2 in all the animals of the groups. However, these findings were observed only in the epineurium (interfascicular connective tissue layer) and in the adjacent adipose tissue of the sciatic nerve (Fig. 4F and G). Likewise, in the epimysium (fibrous tissue envelope that surrounds the skeletal muscle) and in the adipose tissue adjacent to the striated skeletal muscle (Fig. 4J and K, Table S4†), MII score 3 was observed in two animals that received NLC_{CRTL} and NLC_{BTB}.

The promotion of an immune response even with the use of biodegradable nanoparticles is not uncommon prior to their degradation.[24] In this way, the histopathological findings here suggest that after application, the nanoparticles may accumulate externally to the tissues and trigger an inflammatory response aimed at their clearance by the mononuclear phagocyte system.[73] Thus, the results in Fig. 4F, G, J and K may not be related to toxic effects, but to a common inflammatory secondary stimulus, involved in the biodegradation of the nanoparticles. In addition, these findings are encouraging for the advancement of research on this topic, since the accumulation of NLC around the nervous tissue may be the reason for the higher effectiveness and duration of LA-in-NLC (as shown in this work), promoting an efficient delivery to the therapeutic target.

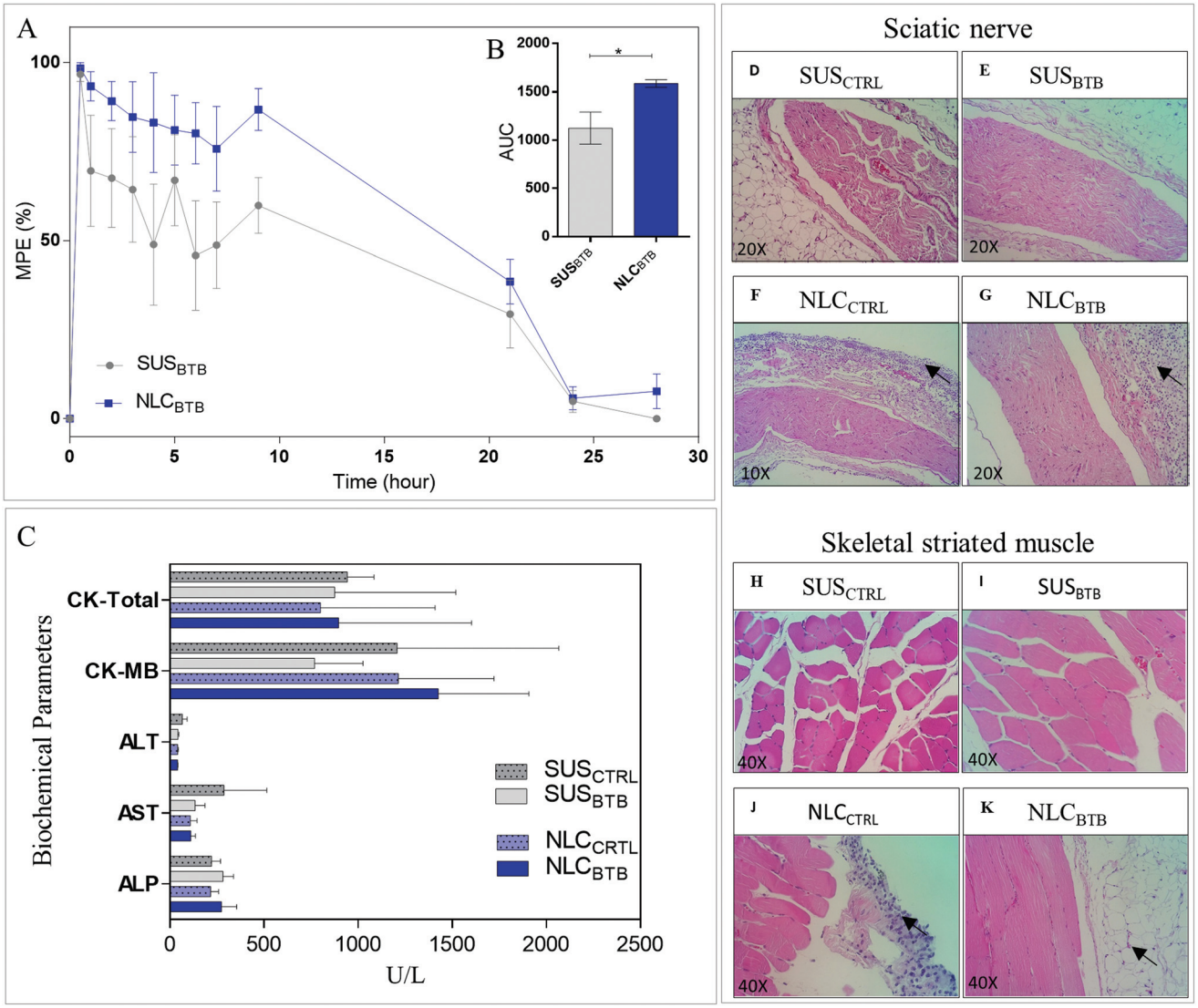

Fig. 4 Anesthetic (PWTP) test. (A) Mean ± SEM of the maximum possible effect (MPE, %) *versus* time; (B) mean ± SEM of the area under the curve (AUC); (C) biochemical parameters of the animal serum after 28 h of formulation injection; and (D–K) relevant histological images of the sciatic nerve and skeletal muscle after 28 h of formulation administration. Some inflammatory cells are noted (arrows). Formulations: suspension of excipients (SUS_{CRTL}) and butamben in suspension (SUS_{BTB}); nanostructured lipid carriers with (NLC_{BTB}) and without (NLC_{CRTL}) butamben. Serum activity of total (CK-total) and cardiac (CK-MB) creatine kinase; alanine aminotransferase (ALT); aspartate aminotransferase (AST); and alkaline phosphatase (ALP) (n = 5). *p < 0.05.

3.4.2. Carrageenan inflammatory hyperalgesia model. Λ-Carrageenan is a polysaccharide commonly used for the study of inflammatory pain, which provides a highly reproducible model for the study of the inflammatory cascade and resulting hyperalgesia.[74] Therefore, it is an appropriate model for the study of the LA effect on inflammatory pain. Following this premise, we evaluated the effects of SUS_{BTB} and NLC_{BTB} in the hyperalgesia induced by carrageenan. Another local anesthetic, articaine (ART), was adopted as a reference because it slightly increases anesthesia at the inflamed tissues.[75]

The hyperalgesia process was accompanied from the time of λ-carrageenan application up to 6 h (Fig. 5A). All treatments were performed 10 min before the time mark of 3 h, which is the period when all inflammatory mediators are present in the inflamed site and act synergistically, with a peak on the experienced pain behavior of the animals.[76] The concentration of LA injected was adjusted to prevent total analgesia, allowing comparisons between the formulations.

The most effective control of hyperalgesia was reached when BTB was used in this model: the reference control, 0.5% ART, showed a 31% decrease in hyperalgesia, while 0.5% BTB in suspension (SUS_{BTB}) and NLC_{BTB} reduced it by 64% and 70%, respectively. Besides, in agreement with the previous tests, the effectiveness of NLC_{BTB} was greater than that of the suspension. Articaine is less liposoluble than BTB and has a pK_a of 7.8,[16] so that the ratio of the neutral/charged ART

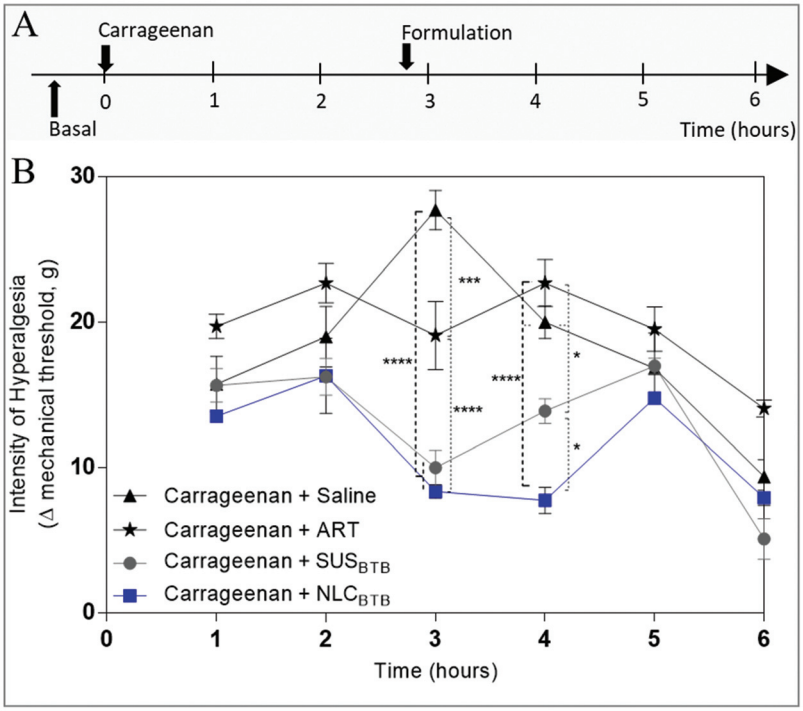

Fig. 5 Carrageenan hyperalgesia model. (A) Experimental design, and (B) mechanical nociceptive threshold measured by the electronic von Frey test, after treatment with saline solution (control), 0.5% articaine (ART; reference), 0.5% BTB in suspension (SUS_{BTB}) or encapsulated into the NLC (NLC_{BTB}). Data are expressed as mean ± SEM of the Δ (delta) mechanical threshold (grams), calculated by subtracting the average measurements from the average basal data. Statistical analysis: two-way ANOVA plus Tukey–Kramer *post hoc* test. * $p < 0.05$, ***$p < 0.001$, ****$p < 0.0001$.

species decreases accordingly to the acidosis caused by the inflammatory process. BTB is not affected by the pH, since it has no ionizable groups at pH > 3. Together, these factors explain the greater effectiveness of BTB over articaine in this inflammatory hyperalgesia model. As expected, the control NLC (without BTB) had no effect in the inflammatory test (data not shown).

Encapsulation of local anesthetics in NLC prolong the anesthetic effect[16] due to the sustained release and also because the nanoparticles protect the encapsulated drug against systemic degradation.[77] Here we showed that also in an inflammatory pain model, the antinociceptive effect of BTB is prolonged when it is encapsulated into these lipid nanoparticles. While the anesthetic effect of SUS_{BTB} and ART decreased after 1 hour of application (4 h after carrageenan administration), NLC_{BTB} retained its effect, keeping the nociceptive response low (Fig. 5B). The capacity of BTB to promote anesthesia under inflammation (improved when loaded in NLC) is really interesting for the post-operative pain control. After 2 h (5 h after carrageenan administration), no more significant anesthetic effect was noticed, for any of the formulations. Additionally, at that moment, the hyperalgesia caused by λ-carrageenan has also decreased by half. These results indicate that NLC_{BTB} has promising advantages for the prospective use in tissues under inflammation. BTB resistance to pH changes bypasses the problem of anesthetic failure due to tissue acidosis, while NLC increase their effectiveness and anesthesia time, in addition to provide a homogeneous formulation of easy application.

4. Conclusion

Butamben encapsulated in NLC proved to be a promising alternative for pain management under inflammatory conditions. The formulation optimized by a factorial design showed desirable properties for parenteral application. The cytotoxicity of this anesthetic agent was reduced when encapsulated and there were no significant systemic changes in the toxicological profile, indicating that the parenteral use of BTB is safe. Finally, in the inflammatory hyperalgesia test, NLC_{BTB} was more effective and showed a greater anesthetic effect than articaine. These encouraging data justify further tests aiming at the clinical application of this DDS, to solve the problem of anesthetic failure under conditions of tissue inflammation.

Author contributions

All authors discussed the results and commented on the manuscript. G. H. R. S.: conceptualization, methodology, data curation, writing/original draft preparation, visualization, resources and investigation; G. G. and L. D. M.: investigation and cryo-EM; F. F. L. and A. C. S.: *in vivo* biochemical and

histological analyses; M. C. B.: conceptualization, validation and writing-review (factorial design, DSC and XDR); J. B. P. L., K. F. M., N. S. C. and C. A. P.: conceptualization, methodology and validation of *in vivo* pain tests and writing/review of the manuscript. E. P.: conceptualization, supervision, project administration, funding acquisition and writing – review and editing.

Conflicts of interest

The authors declare they have no conflict of interest.

Acknowledgements

The authors thank the São Paulo research foundation, FAPESP (G. H. R. S. scholarship #17/15174-5; E. P. grant #14/25372-0), INCT-Bioanalítica (M. C. B. grant) and CAPES (E. P. grant), Dhaymer Ind. Com. Prod. Quim Ltda for kindly providing cetyl palmitate and Dhaykol, and the Brazilian Center for Research in Energy and Materials (CNPEM) for the access to the Cryo-EM facility.

References

1 D. R. de Araujo, E. de Paula and L. F. Fraceto, *Quim. Nova*, 2008, **31**, 1775–1783.
2 A. H. Jeske, in *Contemporary Dental Pharmacology*, ed. A. Jeske, Springer, Cham, 2019, pp. 9–22.
3 E. De Paula, C. M. S. Cereda, G. R. Tofoli, M. Franz-Montan, L. F. Fraceto and D. R. de Araújo, *Recent Pat. Drug Delivery Formulation*, 2010, **4**, 23–34.
4 E. de Paula, C. M. S. Cereda, L. F. Fraceto, D. R. de Araújo, M. Franz-Montan, G. R. Tofoli, J. Ranali, M. C. Volpato and F. C. Groppo, *Expert Opin. Drug Delivery*, 2012, **9**, 1505–1524.
5 C. B. Berde and G. R. Strichartz, in *Miller's Anesthesia*, ed. R. D. Miller, L. I. Eriksson, L. A. Fleisher, J. P. Wiener-Kronish, N. H. Cohen and W. L. Young, Elsevier Ltd, 8th edn, 2016, pp. 1028–1054.
6 T. Ueno, H. Tsuchiya, M. Mizogami and K. Takakura, *J. Inflammation Res.*, 2008, **1**, 41.
7 H. P. Cohen, B. Y. Cha and L. S. W. Spångberg, *J. Endod.*, 1993, **19**, 370–373.
8 I. Potocnik and F. Bajrović, *Endod. Dent. Traumatol.*, 1999, **15**, 247–251.
9 S. Kattan, S. M. Lee, E. V. Hersh and B. Karabucak, *J. Am. Dent. Assoc.*, 2019, **150**, 165–177.
10 S. F. Malamed, *Handbook of local anesthesia*, Elsevier, 2013.
11 J. H. Goodchild and M. Donaldson, *Compend. Contin. Educ. Dent.*, 2016, **37**, e6–e12.
12 R. A. Christoph, L. Buchanan, K. Begalla and S. Schwartz, *Ann. Emerg. Med.*, 1988, **17**, 117–120.
13 F. P. Buckley, G. D. Neto and B. R. Fink, *Anesth. Analg.*, 1985, **64**, 477–482.
14 J. Larocca de Geus, J. K. Nogueira da Costa, L. M. Wambier, B. M. Maran, A. D. Loguercio and A. Reis, *J. Am. Dent. Assoc.*, 2020, **151**, 87–97.
15 G. J. Grant, J. Lax, L. Susser, M. Zakowski, T. E. Weissman and H. Turndorf, *Acta Anaesthesiol. Scand.*, 1997, **41**, 204–207.
16 D. R. de Araújo, L. N. de M. Ribeiro and E. de Paula, *Expert Opin. Drug Delivery*, 2019, **16**, 701–714.
17 C. Lottinger and J. McNeish, in *Office-Based Maxillofacial Surgical Procedures*, Springer International Publishing, Cham, 2019, pp. 65–85.
18 M. Shulman, T. R. Lubenow, H. A. Nath, W. Blazek, R. J. Mccarthy, D. Pharm and A. D. Ivankovich, *Reg. Anesth. Pain Med.*, 1998, **23**, 395–401.
19 Y. A. Kolesnikov, M. Cristea and G. W. Pasternak, *Anesth. Analg.*, 2003, **97**, 1103–1107, table of contents.
20 L. J. A. Rampaart, J. P. Beekwilder, G. T. H. Van Kempen, R. J. Van Den Berg and D. L. Ypey, *Anesth. Analg.*, 2008, **106**, 1778–1783.
21 C. M. S. Cereda, M. Franz-Montan, C. M. G. Da Silva, B. R. Casadei, C. C. Domingues, G. R. Tofoli, D. R. De Araujo and E. De Paula, *J. Liposome Res.*, 2013, **23**, 228–234.
22 M. Svärd, L. Zeng, M. Valavi, G. R. Krishna and Å. C. Rasmuson, *J. Pharm. Sci.*, 2019, **108**, 2377–2382.
23 Food and Drug Administration, *List of Drug Products That Have Been Withdrawn or Removed From the Market for Reasons of Safety or Effectiveness*, 1998, vol. 63.
24 R. H. Muller, R. Shegokar and C. M. Keck, *Curr. Drug Discovery Technol.*, 2011, **8**, 207–227.
25 E. B. Souto, I. Baldim, W. P. Oliveira, R. Rao, N. Yadav, F. M. Gama and S. Mahant, *Expert Opin. Drug Delivery*, 2020, **17**, 357–377.
26 C. Carbone, B. Tomasello, B. Ruozi, M. Renis and G. Puglisi, *Eur. J. Med. Chem.*, 2012, **49**, 110–117.
27 G. H. Rodrigues da Silva, L. N. M. Ribeiro, H. Mitsutake, V. A. Guilherme, S. R. Castro, R. J. Poppi, M. C. Breitkreitz and E. de Paula, *Int. J. Pharm.*, 2017, **529**, 253–263.
28 C. A. Schneider, W. S. Rasband and K. W. Eliceiri, *Nat. Methods*, 2012, **9**, 671–675.
29 R. J. McCarthy, J. M. Kerns, H. A. Nath, M. Shulman and A. D. Ivankovich, *Anesth. Analg.*, 2002, **94**, 711–716; table of contents.
30 A. Mendyk, R. Jachowicz, K. Fijorek, P. Doro, P. Kulinowski, S. Polak, P. Dorożyński, P. Kulinowski and S. Polak, *Dissolution Technol.*, 2012, 6–11.
31 K. H. Ramteke, P. A. Dighe, A. Kharat and S. V. Patil, *Scholars Acad. J. Pharm.*, 2014, **3**, 2320–4206.
32 A. A. Welder, *Toxicology*, 1992, **72**, 175–187.
33 N. F. S. de Melo, R. Grillo, V. A. Guilherme, D. R. de Araujo, E. de Paula, A. H. Rosa and L. F. Fraceto, *Pharm. Res.*, 2011, **28**, 1984–1994.
34 L. O. Randall and J. J. Selitto, *Arch. Int. Pharmacodyn. Ther.*, 1957, **CXI**, 409–419.
35 J. P. Penning and T. L. Yaksh, *Anesthesiology*, 1992, **77**, 1186–2000.
36 O. N. K. Martey, G. Armah and L. K. N.-A. Okine, *Afr. J. Tradit., Complementary Altern. Med.*, 2010, **7**, 231–240.

37 W. Zink, J. R. E. Bohl, N. Hacke, B. Sinner, E. Martin and B. M. Graf, *Anesth. Analg.*, 2005, **101**, 548–554.
38 H. Dyhre, L. Söderberg, S. Björkman and C. Carlsson, *Reg. Anesth. Pain Med.*, 2006, **31**, 401–408.
39 G. G. Vivancos, W. A. Verri, T. M. Cunha, I. R. S. Schivo, C. A. Parada, F. Q. Cunha and S. H. Ferreira, *Braz. J. Med. Biol. Res.*, 2004, **37**, 391–399.
40 J. das Neves and B. Sarmento, *Acta Biomater.*, 2015, **18**, 77–87.
41 M. Pradhan, D. Singh, S. N. Murthy and M. R. Singh, *Steroids*, 2015, **101**, 56–63.
42 S. Das, W. K. Ng and R. B. H. Tan, *Eur. J. Pharm. Sci.*, 2012, **47**, 139–151.
43 Z. Rahman, A. S. Zidan and M. A. Khan, *Eur. J. Pharm. Biopharm.*, 2010, **76**, 127–137.
44 L. N. M. Ribeiro, M. C. Breitkreitz, V. A. Guilherme, G. H. R. da Silva, V. M. Couto, S. R. Castro, B. O. de Paula, D. Machado and E. de Paula, *Eur. J. Pharm. Sci.*, 2017, **106**, 102–112.
45 H. Chen, Y. Wang, Y. Zhai, G. Zhai, Z. Wang and J. Liu, *Colloids Surf., A*, 2015, **465**, 130–136.
46 X. Zhang, J. Liu, H. Qiao, H. Liu, J. Ni, W. Zhang and Y. Shi, *Powder Technol.*, 2010, **197**, 120–128.
47 S. Zhao, X. Yang, V. M. Garamus, U. A. Handge, L. Bérengère, L. Zhao, G. Salamon, R. Willumeit, A. Zou and S. Fan, *Langmuir*, 2014, **30**, 6920–6928.
48 E. Lasoń, E. Sikora and J. Ogonowski, *Acta Biochim. Pol.*, 2013, **60**, 773–777.
49 F. Han, S. Li, R. Yin, H. Liu and L. Xu, *Colloids Surf., A*, 2008, **315**, 210–216.
50 R. H. Müller, K. Mäder and S. Gohla, *Eur. J. Pharm. Biopharm.*, 2000, **50**, 161–177.
51 S. Doktorovová, A. B. Kovačević, M. L. Garcia and E. B. Souto, *Eur. J. Pharm. Biopharm.*, 2016, **108**, 235–252.
52 A. Gordillo-Galeano and C. E. Mora-Huertas, *Eur. J. Pharm. Biopharm.*, 2018, **133**, 285–308.
53 K. Jores, W. Mehnert, M. Drechsler, H. Bunjes, C. Johann and K. Mäder, *J. Controlled Release*, 2004, **95**, 217–227.
54 F. Maestrelli, M. L. L. González-Rodríguez, A. M. M. Rabasco, C. Ghelardini and P. Mura, *Int. J. Pharm.*, 2010, **395**, 222–231.
55 E. Gonzalez-Mira, M. A. A. Egea, M. L. L. Garcia and E. B. B. Souto, *Colloids Surf., B*, 2010, **81**, 412–421.
56 V. A. Guilherme, L. N. M. Ribeiro, A. C. S. Alcântara, S. R. Castro, G. H. Rodrigues da Silva, C. G. da Silva, M. C. Breitkreitz, J. Clemente-Napimoga, C. G. Macedo, H. B. Abdalla, R. Bonfante, C. M. S. S. Cereda and E. de Paula, *Sci. Rep.*, 2019, **9**, 11160.
57 R. H. Müller, U. Alexiev, P. Sinambela and C. M. Keck, in *Percutaneous Penetration Enhancers Chemical Methods in Penetration Enhancement*, Springer Berlin Heidelberg, Berlin, Heidelberg, 2016, pp. 161–185.
58 L. N. M. Ribeiro, M. Franz-Montan, M. C. Breitkreitz, A. C. S. Alcântara, S. R. Castro, V. A. Guilherme, R. M. Barbosa and E. de Paula, *Eur. J. Pharm. Sci.*, 2016, **93**, 192–202.
59 G. H. Rodrigues da Silva, G. Geronimo, L. N. M. Ribeiro, V. A. Guilherme, L. D. de Moura, A. L. Bombeiro, J. D. Oliveira, M. C. Breitkreitz and E. de Paula, *Mater. Sci. Eng., C*, 2020, **109**, 110608.
60 R. Perez-Castro, S. Patel, Z. V. Garavito-Aguilar, A. Rosenberg, E. Recio-Pinto, J. Zhang, T. J. J. Blanck and F. Xu, *Anesth. Analg.*, 2009, **108**, 997–1007.
61 I. A. M. Radwan, S. Saito and F. Goto, *Anesth. Analg.*, 2002, **94**, 319–324.
62 R. M. Barbosa, C. M. G. da Silva, T. S. Bella, D. R. de Araújo, P. D. Marcato, N. Durán and E. de Paula, *J. Phys.: Conf. Ser.*, 2013, **429**, 012035.
63 D. M. Ridolfi, P. D. Marcato, D. Machado, R. A. Silva, G. Z. Justo and N. Durán, *J. Phys.: Conf. Ser.*, 2011, **304**, 012032.
64 N. Schöler, E. Zimmermann, U. Katzfey, H. Hahn, R. H. Müller and O. Liesenfeld, *Int. J. Pharm.*, 2000, **196**, 235–239.
65 C. J. Sinnott and G. R. Strichartz, *Reg. Anesth. Pain Med.*, 2003, **28**, 294–303.
66 C. M. S. Cereda, G. R. Tofoli, L. G. Maturana, A. Pierucci, L. A. S. Nunes, M. Franz-Montan, A. L. R. Oliveira, S. Arana, D. R. de Araujo and E. de Paula, *Anesth. Analg.*, 2012, **115**, 1234–1241.
67 Y. Krishnan, S. Mukundan, S. Akhil, S. Gupta and V. Viswanad, *Adv. Pharm. Bull.*, 2018, **8**, 257–265.
68 A. H. Foster and B. M. Carlson, *Anesth. Analg.*, 1980, **59**, 727–736.
69 R. Tiwari and K. Pathak, *Int. J. Pharm.*, 2011, **415**, 232–243.
70 E. Esposito, H. E. De Vries, S. M. A. van der Pol, F. Boschi, L. Calderan, S. Mannucci, M. Drechsler, C. Contado, R. Cortesi and C. Nastruzzi, *J. Nanomed. Nanotechnol.*, 2015, **6**(1), 1000256.
71 Y. Zhao, L. Wang, M. Yan, Y. Ma, G. Zang, Z. She and Y. Deng, *Int. J. Nanomed.*, 2012, **7**, 2891–2900.
72 V. Pokharkar, A. Patil-Gadhe and P. Palla, *Biomed. Pharmacother.*, 2017, **94**, 150–164.
73 F. Alexis, E. Pridgen, L. K. Molnar and O. C. Farokhzad, in *Molecular Pharmaceutics*, American Chemical Society, 2008, vol. 5, pp. 505–515.
74 T. M. Cunha, W. A. Verri, J. S. Silva, S. Poole, F. Q. Cunha and S. H. Ferreira, *Proc. Natl. Acad. Sci. U. S. A.*, 2005, **102**, 1755–1760.
75 V. Nagendrababu, H. F. Duncan, J. Whitworth, M. H. Nekoofar, S. J. Pulikkotil, S. K. Veettil and P. M. H. Dummer, *Int. Endod. J.*, 2020, **53**, 200–213.
76 K. R. Patil and C. R. Patil, *J. Tradit., Complementary Med.*, 2017, **7**, 86–93.
77 P. Severino, T. Andreani, A. S. Macedo, J. F. Fangueiro, M. H. A. Santana, A. M. Silva and E. B. Souto, *J. Drug Delivery*, 2012, **2012**, 750891.